# Selective Inhibition of Cysteine-Dependent Enzymes by Bioorthogonal Tethering

**Luke A. Spear [1], Yang Huang [2], Jinghao Chen [2], Alexander R. Nödling [1], Satpal Virdee [3]* and Yu-Hsuan Tsai [1,2]***

*1 - **School of Chemistry,** Cardiff University, Cardiff, United Kingdom*
*2 - **Institute of Molecular Physiology,** Shenzhen Bay Laboratory, Shenzhen, China*
*3 - **MRC Protein Phosphorylation and Ubiquitylation Unit,** University of Dundee, Dundee, United Kingdom*

***Correspondence to Satpal Virdee and Yu-Hsuan Tsai:** s.s.virdee@dundee.ac.uk (S. Virdee), Tsai.Y-H@outlook.com (Y.-H. Tsai),*
https://doi.org/10.1016/j.jmb.2022.167524
***Edited by Tao Liu***

## Abstract

A general approach for the rapid and selective inhibition of enzymes in cells using a common tool compound would be of great value for research and therapeutic development. We previously reported a chemogenetic strategy that addresses this challenge for kinases, relying on bioorthogonal tethering of a pan inhibitor to a target kinase through a genetically encoded non-canonical amino acid. However, pan inhibitors are not available for many enzyme classes. Here, we expand the scope of the chemogenetic strategy to cysteine-dependent enzymes by bioorthogonal tethering of electrophilic warheads. For proof of concept, selective inhibition of two E2 ubiquitin-conjugating enzymes, UBE2L3 and UBE2D1, was demonstrated in biochemical assays. Further development and optimization of this approach should enable its use in cells as well as with other cysteine-dependent enzymes, facilitating the investigation of their cellular function and validation as therapeutic targets.


## Introduction

Regulated enzyme activity is critical to our health, and aberrant activation is associated with many human diseases.[1–3] However, the cellular function, and hence therapeutic potential, of many enzymes remains largely unexplored. Although advances in genomic techniques have revealed statistical correlation between enzyme mutations (or altered expression) and a large number of diseases, they do not tell us whether aberrant enzyme activity is a driver of the diseases.[4] In addition, thousands of human enzymes remain uncharacterized,[5] and thus their cellular functions and disease relevance are unknown. Given the importance of enzymes to our wellbeing, there is a great impetus to decrypt these unknowns. In particular, assigning physiological functions to enzymes is a major goal in the post-genomics era.

A powerful method for investigating physiological enzyme activity, and assessing the therapeutic potential of its modulation, is to inhibit enzymes of interest selectively and rapidly with a small-molecule tool compound. However, potent and selective compounds are only available for a minor fraction of the proteome and typically require costly development involving the screening of large compound libraries followed by multiple rounds of optimization, with no guarantee of success.[6,7] Genetic approaches, such as gene knockdown and knockout, are powerful means to specifically interrogate the function of, in principle, any enzyme in the cell.[8] However, genetic approaches are associated with a long lag time

such that cells can establish compensatory mechanisms masking the biological phenomenon under investigation.[9] Furthermore, enzymes can be extremely large and have additional non-catalytic functions which knockdown and knockout approaches do not enable deconvolution from. In contrast, chemical or pharmacological inhibition of enzymes by small molecules can normally be achieved within minutes, providing high temporal resolution to the analysis of the biological processes.[10]

Chemogenetic inhibition combines the advantages of both genetic (i.e., specific) and chemical (i.e., rapid) approaches.[11,12] Here, a genetic modification is introduced into the enzyme of interest, a process known as "sensitization", so that the target enzyme becomes sensitive to a designer small molecule derived from an inhibitor that has no discernible selectivity towards the wild-type enzyme or its closely related family members. The most prominent example is the "bump-and-hole" strategy for selective inhibition of kinases. Here the sensitized variant can be generated by mutating a conserved, bulky amino acid residue in the active site to create a "hole" that is complemented by a steric "bump" designed into the pan inhibitor.[11] However, this approach is not applicable to some kinases, as mutation of the conserved amino acid residue abolishes their activity.[13]

We developed a complementary approach to the bump-and-hole strategy for selective kinase inhibition involving bioorthogonal ligand tethering (Figure 1(A)).[14] In this approach, a sensitized target is generated by placing a non-canonical amino acid bearing bioorthogonal functionality in proximity to the enzyme active site through genetic code expansion. A known pan inhibitor is then repurposed by derivatizing it with the complementary bioorthogonal group. Central to this strategy is the high second order rate constant demonstrated by biorthogonal inverse electron demand Diels-Alder chemistry that enables efficient tethering when the inhibitor conjugate is administered at concentrations that nominally would be sub-inhibitory. Thus, the sensitized target can be selectively inhibited by the inhibitor conjugate due to covalent tethering. Using this approach, selective and rapid inhibition of intracellular kinases CRAF, MEK1, MEK2 and LCK, for which no selective small-molecule inhibitors exist, can be achieved.[14,15] However, both chemogenetic approaches rely on repurposing a known inhibitor, which is unfortunately not available for many enzymes.[7]

A strategy to develop a more general approach for selective and rapid inhibition of any enzyme is to explore covalent modification of nucleophilic active site residues displayed by an enzyme class, instead of repurposing known inhibitors. Therefore, it will be possible to achieve selective and rapid inhibition, even of enzymes that are poorly characterized. To this end, we explored the feasibility of targeting the hundreds of enzymes that contain a catalytically important cysteine nucleophile for selective and rapid inhibition.

The thiol functional group of a catalytically important cysteine residues is indispensable for the enzyme activity, so its covalent modification will inevitably abolish the enzymatic function. We hypothesized that this could be achieved by tethering a small-molecule conjugate, which contains a proximity-dependent thiol-reactive electrophilic warhead, to the target enzyme (Figure 1(B)). Like our recent approach for kinase inhibition (Figure 1(A)),[14] the sensitized target will contain a bioorthogonal amino acid (**1**, Figure 1 (C)), and the inhibitor conjugate will bear the complementary bioorthogonal group, tetrazine (Figure 1 (D)), that undergoes rapid reaction with the cyclopropene functionality on **1** ($k \sim 10\ M^{-1}\ s^{-1}$,[16] Figure 1(E)). We chose to use cyclopropene lysine **1** for bioorthogonal tethering based on two reasons. Firstly, incorporation efficiency of cyclopropene lysine in mammalian cells is higher than that of other tetrazine-reactive bioorthogonal amino acids.[17] Secondly, we were able to achieve selective tethering and inhibition of cyclopropene-containing LCK kinase in mammalian cells after incubation with culture media containing a tetrazine-bearing conjugate at 1 μM within 20 min.[14] On the other hand, the low reactivity of the proximity-dependent thiol-reactive warheads ($k = 10^{-2}$ to $10^{-3}\ M^{-1}\ s^{-1}$) means that with both reactants at single digit micromolar concentrations, the half-life of diffusion-driven cysteine reactivity is on a time scale of months or even years, but could be proximity-accelerated by up to 5-orders of magnitude.[18] The conjugate is therefore expected to exhibit high specificity in inhibiting the target enzyme and have negligible off-target activity in cells.

## Results

### Design of inhibitor conjugates

We synthesized conjugates **2-8** (Figure 1(G)) carrying a tetrazine functionality, so that it can undergo bioorthogonal tethering to cyclopropene lysine **1** on the sensitized target protein. Among different 3,6-disubstituted-1,2,4,5-tetrazines characterized to date, those with proton (H) and phenyl (Ph) substituents are known to have superior reaction kinetics and commonly employed to generate cell-permeable probes.[19–21] For these reasons, we generated tetrazine conjugates based on these motifs.

As a negative control, conjugate **2** contains a bulky and unreactive *tert*-butyloxycarbonyl group instead of a thiol-reactive warhead. Conjugates **3-8** contain a warhead that should undergo chemoselective reactions with thiols.[18,22–24] Specifically, conjugates **3** and **4** contain a weakly thiol-reactive Michael acceptor. Conjugates **5-7** contain a chloroacetyl warhead with an alkyl or an

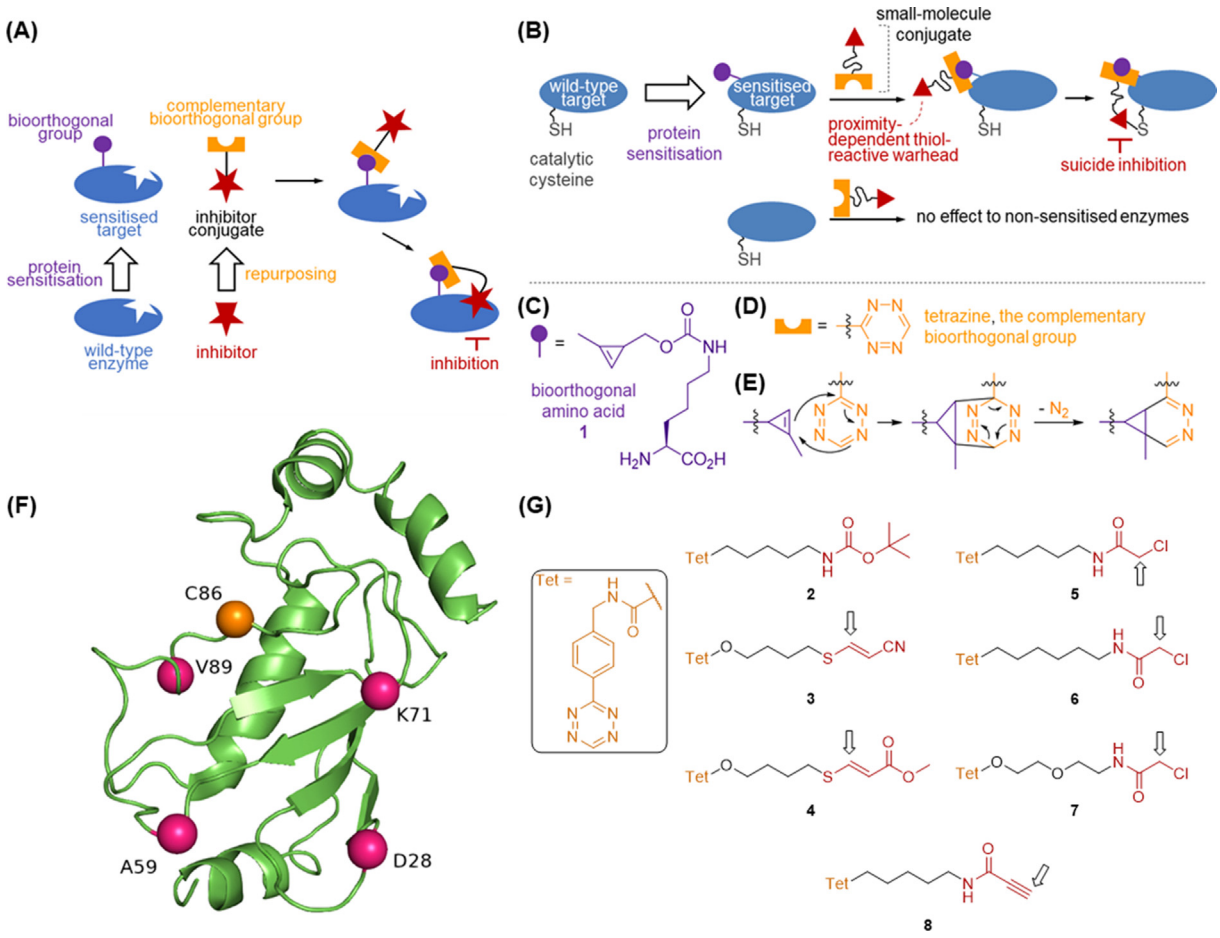


**Figure 1. (A)** Chemogenetic inhibition by bioorthogonal ligand tethering. **(B)** Selective inhibition of a cysteine-dependent enzyme. The small molecule conjugate is expected to only inhibit the sensitized target but has no effect to the wild-type and any non-sensitized enzymes at the concentration it is administered at. **(C)** Structure of bioorthogonal amino acid **1** for protein sensitization. **(D)** Structure of the complementary bioorthogonal group, tetrazine, on the small-molecule conjugate. **(E)** Mechanism of the inverse electron demand Diels-Alder reaction between cyclopropene on **1** and tetrazine on the small-molecule conjugate used for bioorthogonal tethering. **(F)** Structure of UBE2L3, highlighting the catalytic cysteine residue (C86) and residues to be substituted with **1**. PDB: 1C4Z. **(G)** Structure of designed inhibitor conjugates **2-8**. The atom for nucleophilic attachment by the active site thiol group is indicated with an arrow.

ethylene glycol linker. Conjugate **8** contains a propiolamide that can also be seen as a Michael acceptor. It is noteworthy that the number of atoms in the linker region between the tetrazine and the electrophilic carbon atom among conjugates **6-8** is the same.

## Identification of functional UBE2L3 variants containing a bioorthogonal amino acid

For proof of concept, we used E2 ubiquitin conjugating enzyme, UBE2L3, as the model enzyme. In humans, there are ~35 E2 enzymes. These enzymes are believed to play critical roles in different diseases[25] but have yet to be thoroughly characterized due to the lack of appropriate methods.[26] UBE2L3 is one of the E2 enzymes with structural and biochemical information available,[25] which are useful for establishing the proposed method. Specifically, UBE2L3(C17S/C137S), where the non-catalytic cysteine residues are mutated to serine, is still functional (Figure 2).[27] We name this variant UBE2L3*, which serves as a simple model to verify our hypothesis as this variant contains only one cysteine residue. Based on the crystal structure of UBE2L3,[28] four residues (D28, A59, K71, and V89) were selected for replacement with the bioorthogonal amino acid **1** using the technique of genetic code expansion,[29,30] generating UBE2L3* (XX-**1**) variants where XX denotes the amino acid residue to be replaced (Figure 1(F)). The selected residues are within 24 Å of the catalytic cysteine residue (C86), and this distance is within the maximum theoretical distance (*ca.* 35 Å) if **1** and cysteine side chains are connected by one of our conjugates.

All UBE2L3* variants were recombinantly produced in *E. coli* and purified by affinity

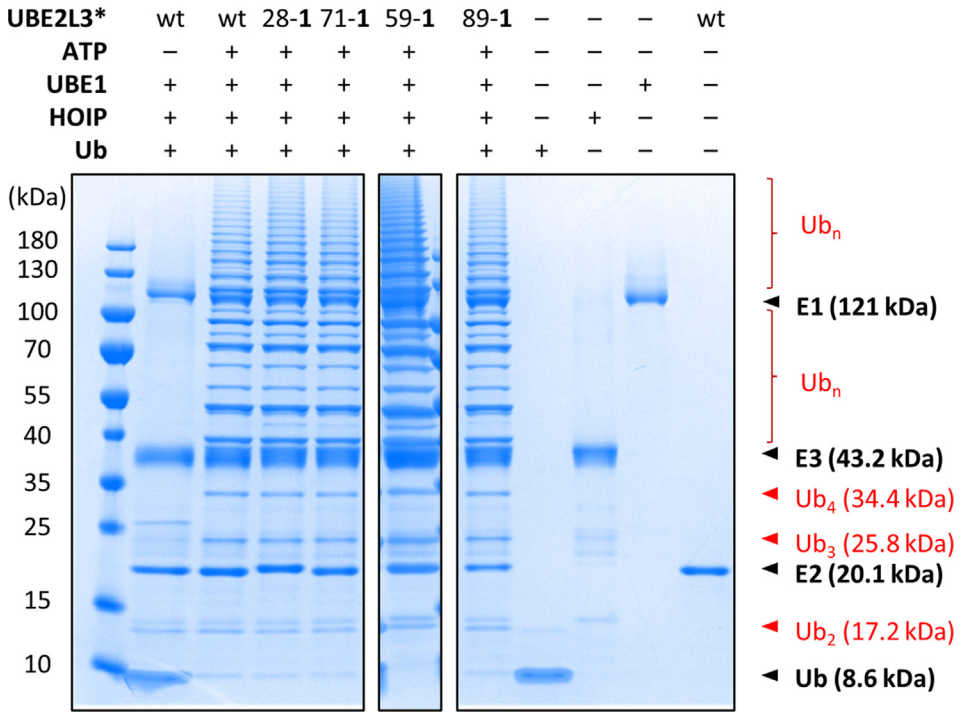


**Figure 2.** UBE2L3*(XX-**1**) variants are functional. SDS-PAGE analysis of the formation of linear ubiquitin chains in the presence of E1 (UBE1), E2 (UBE2L3), E3 (HOIP), ubiquitin (Ub) and ATP. In the absence of ATP, no polyubiquitin chains were formed.

chromatography. Activity of the variants was confirmed using a polyubiquitination assay monitored by SDS-PAGE. The assay tracks the formation of linear polyubiquitin chains and the consumption of ubiquitin monomers via the combined activity of E1-activating enzyme (UBE1), E2-conjugating enzyme (UBE2L3) and E3 ligase (HOIP) in the presence of ATP.[31] In the presence of functional UBE2L3, ubiquitin monomers are expected to be polymerized into ubiquitin chains, and this was the case for all UBE2L3*(XX-**1**) variants (Figure 2).

## Selective inhibition of UBE2L3*(XX-1) variants

To assess if conjugates **2-8** are able to inhibit the activity of UBE2L3*(XX-**1**) variants, individual variants were incubated with a 10-fold excess of a conjugate for 16 h to ensure complete bioorthogonal tethering and then subjected to the polyubiquitination assay.

The reaction of cyclopropene and tetrazine has a rate constant around 2 $M^{-1}$ $s^{-1}$ (Supplementary Figure 1), in agreement with the literature values,[16] and the reaction time can be reduced to 4 h (Supplementary Figure 2). Further reduction in reaction time and stoichiometry of the conjugate should be attainable through employment of a more reactive amino acid, such as exo-bicyclo[6.1.0]nonyne lysine, of which 5 μM can react with equimolar tetrazine completely within a few minutes (Supplementary Figure 2).

In the polyubiquitination assay, none of the conjugates showed any inhibitory effect on UBE2L3* that did not contain bioorthogonal amino acid **1**, demonstrating the lack of tethering-independent modification of thiol functionality on UBE1, non-sensitized UBE2L3 or HOIP (Supplementary Figure 3). While activity of variants 28-**1**, 59-**1** and 71-**1** did not seem to be affected by any conjugates (Figure 3(A) and Supplementary Figure 3), conjugate **7** significantly reduced the level of polyubiquitination supported by UBE2L3*(89-**1**) (Figure 3(B) and Supplementary Figure 4). Mass spectrometry confirmed bioorthogonal tethering of **7** to both 28-**1** and 89-**1** variants (Figure 3(C)–(E)). However, covalent modification of the catalytic cysteine residue was only observed in UBE2L3*(89-**1**) but not UBE2L3*(28-**1**). This is likely due to the longer distance of the tethering site to the catalytic cysteine residue in UBE2L3*(28-**1**). It is also noteworthy that the conjugate also seemed to be inert to 50 mM glutathione (Supplementary Figure 5), confirming the proximity dependence of the warhead. Taken together, we believe the selective inhibition of UBE2L3*(89-**1**) by **7** resulted from bioorthogonal tethering and subsequent proximity-dependent cysteine modification.

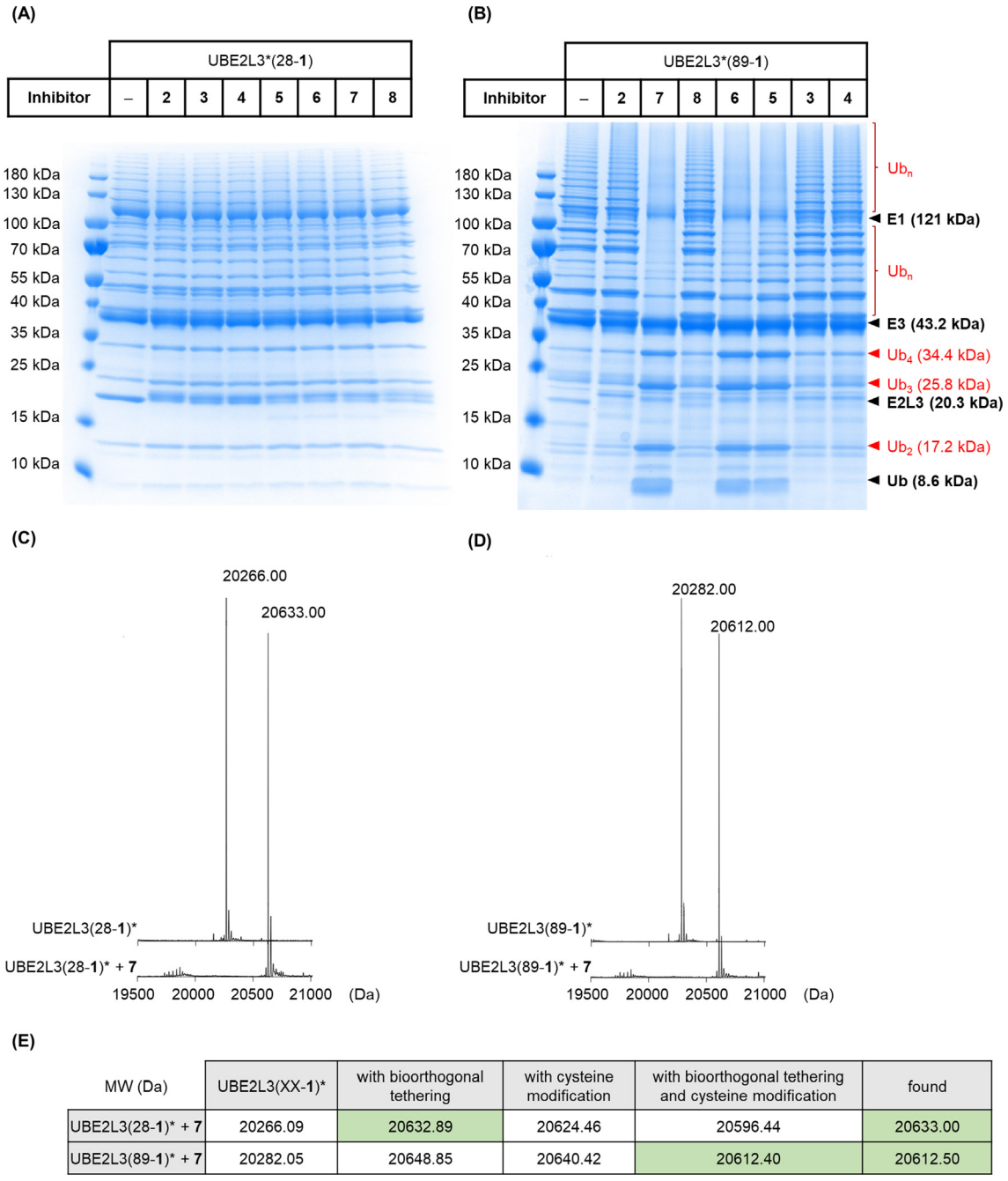


(E)

| MW (Da) | UBE2L3(XX-1)* | with bioorthogonal tethering | with cysteine modification | with bioorthogonal tethering and cysteine modification | found |
|---|---|---|---|---|---|
| UBE2L3(28-1)* + 7 | 20266.09 | 20632.89 | 20624.46 | 20596.44 | 20633.00 |
| UBE2L3(89-1)* + 7 | 20282.05 | 20648.85 | 20640.42 | 20612.40 | 20612.50 |

**Figure 3.** Selective inhibition of UBE2L3*(XX-**1**) by pre-incubation with 50 μM conjugate. Dimethyl sulfoxide (DMSO) was used as the negative control (–). **(A)** Conjugates **2-8** did not show any observable effect on the activity of UBE2L3*(28-**1**). **(B)** Activity of UBE2L3*(89-**1**) can be inhibited to varying degrees by prior incubation with conjugate **5**, **6** or **7**. **(C)** Mass spectrometry analysis showing the product of bioorthogonal reaction between conjugate **7** and UBE2L3*(28-**1**) but no cysteine modification. **(D)** The same reaction with UBE2L3*(89-**1**) indicated bioorthogonal tethering and covalent modification of the catalytic cysteine residue. **(E)** Expected and observed molecular weight of samples under different conditions.

## Re-introduction of non-catalytic cysteine residues in UBE2L3

With the initial success, we wondered if the presence of non-catalytic cysteine residues would interfere with the enzyme inhibition. Thus, we re-introduced the two non-catalytic cysteine residues, C17 and C137, generating the wild-type like variant, UBE2L3(89-**1**). Activity of wild-type UBE2L3 is consistent with the literature[31] and was not affected by conjugate **7**, whereas ubiquitin turnover was successfully inhibited for UBE2L3(89-**1**) pre-incubated with **7** (Figure 4(A)), indicating the

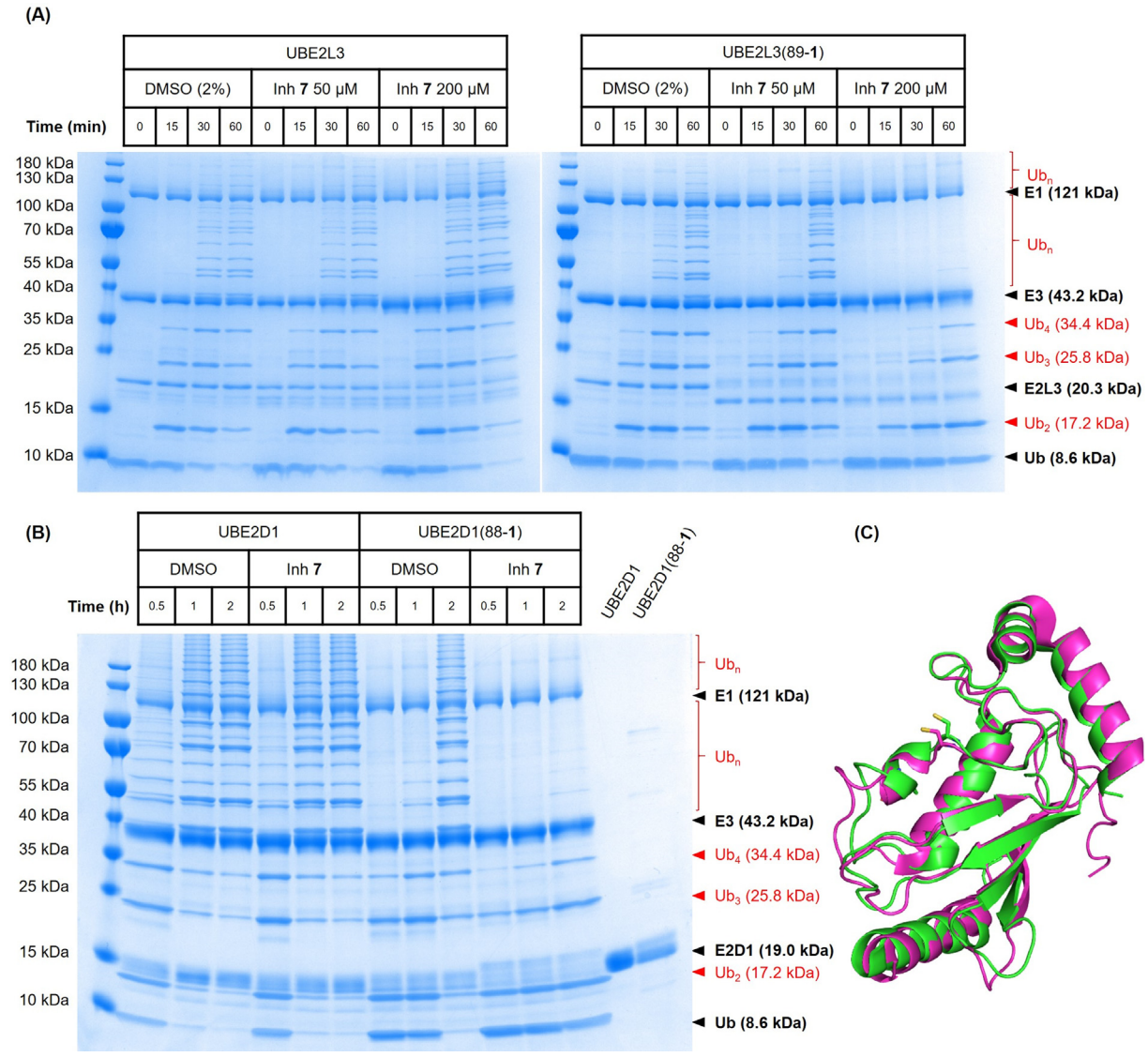


**Figure 4.** **(A)** Polyubiquitination assay after pre-incubation with conjugate **7** or a DMSO control for both the UBE2L3 wild-type and UBE2L3(89-**1**) after re-introduction of native cysteines at amino acid positions 18 and 137. **(B)** Inhibitor assay showing activity of UBE2D1(88-**1**) is hindered by conjugate **7**. DMSO is used as the control in reactions with no inhibitor. **(C)** Structural alignment of UBE2L3 (pink, PDB: 4Q5E) and UBE2D1 (green, PDB: 6D4P).

presence of the non-catalytic cysteine residues does not affect enzyme inhibition. Mass spectrometry also confirmed the bioorthogonal tethering of the conjugate **7** and covalent modification of a cysteine residue (Supplementary Figure 6).

## Selective inhibition of UBE2D1

To evaluate the general applicability of this strategy, we put bioorthogonal amino acid **1** into another E2 enzyme, UBE2D1, containing both catalytic and non-catalytic cysteine residues. While UBE2D1 has only 39% sequence identity to UBE2L3, it can also be employed together with UBE1 and HOIP to form polyubiquitin chains in the presence of ATP (Figure 4(B)).[25] UBE2D1(88-**1**) has the bioorthogonal amino acid at the homologous position to UBE2L3(89-**1**), according to both sequence and structural alignment (Figure 4(C)). Gratifyingly, conjugate **7** had no effect on wild-type UBE2D1 but could effectively inhibit UBE2D1 (88-**1**), demonstrating the transferability of this strategy.

## Cell permeability of conjugates 6 and 7

For cellular applications, conjugates have to be cell permeable, and we evaluated the cell permeability of conjugates **6** and **7** using a kinase reporter assay. HEK293T cells expressing constitutively active MEK1(76-**1**) have high level of phosphorylated ERK, but the activity of MEK1(76-**1**) can be inhibited by tetrazine derivative **9** of a MEK1/2 inhibitor (Supplementary Figure 7).[14] We

thus incubated cells with **6** or **7**, followed by treatment with MEK1/2 inhibitor conjugate **9**. If conjugate **6** or **7** is cell permeable, it would be covalently attached to MEK1(76-**1**), preventing tethering of **9**, so the kinase should remain active. On the other hand, if conjugate **6** or **7** is not cell permeable, subsequent treatment with **9** would inhibit the activity of MEK1(76-**1**). To our disappointment, MEK1(76-**1**)-expressing cells subjected to sequential treatment of **6**/**7** and **9** showed significantly lower level of phosphorylated ERK than non-treated cells or cells treated with **6** or **7** only (Supplementary Figure 7), indicating conjugates **6** and **7** are unlikely to be cell permeable. We also performed the assay using a more reactive MEK1 variant containing a bicyclo[6.1.0]nonyne lysine **10**, and the observation remained the same. On the other hand, treatment of MEK1 variant with *N*-Boc 4-(1,2,4,5-tetrazin-3-yl)benzylamine **11** first indeed prevented subsequent tethering of **9**, validating the suitability of this assay for assessing cell permeability (Supplementary Figure 7).

## Discussion

We have demonstrated the feasibility of selective enzyme inhibition through covalent modification of the catalytic cysteine residue. Our chemogenetic approach employs genetic code expansion to incorporate a non-canonical amino acid bearing a bioorthogonal group, enabling tethering of a proximity-dependent thiol-reactive warhead. Here, we chose to use cyclopropene lysine **1** for bioorthogonal tethering due to its high incorporation efficiency in mammalian cells[17] and our previous success in rapidly inhibiting cyclopropene-containing LCK kinase in mammalian cells.[14] However, previous conjugates utilized for kinase inhibition were derived from known kinase inhibitors,[14] so these conjugates are likely to have some affinity to the target kinase, facilitating bioorthogonal tethering. On the other hand, conjugates prepared in this study were not derived from any ligand or E2 binder, and the tethering kinetics seem to solely depend on the rate of the employed bioorthogonal reaction. Indeed, much higher concentration of the conjugate (50 vs 1 μM) and much longer reaction time (16 vs 2 h) were employed in the polyubiquitination assays. Moving forwards, it would be beneficial to use a more reactive bioorthogonal amino acid, such as bicyclo[6.1.0]nonyne lysine **10** (Supplementary Figure 2), so that complete tethering can be achieved with lower concentration of the conjugate in less time. This is also evident in the cell permeability investigation, where tetrazine **11** efficiently blocked the MEK1 variant containing a bicyclo[6.1.0]nonyne lysine but not cyclopropene lysine for subsequent tethering with MEK1/2 inhibitor conjugate **9** (Supplementary Figure 7).

Central to this chemogenetic approach for selective inhibition of cysteine-dependent enzymes is the tethering-based proximity-dependent modification of the catalytic cysteine residue. To achieve selective inhibition, both the position of the bioorthogonal amino acid and the structure of the conjugate are important as inhibition was most prominent in UBE2L3*(89-**1**) variants treated with conjugate **7**, which did not seem to affect the activity of other variants (Supplementary Figure 3). Moreover, inhibition of UBE2L3*(89-**1**) by conjugate **6**, where two oxygen atoms on the linker of **7** are replaced with carbon atoms, was less effective than **7**.

While mass spectrometry indicated complete bioorthogonal tethering and cysteine modification of **7**-treated UBE2L3*(89-**1**), there are still some observable bands corresponding to polyubiquitin chains (Figure 3(B)). One possibility is that there may still be a trace amount of unmodified enzyme, not detected by mass spectrometry, participating in the formation of polyubiquitin chains. Another possibility is due to the presence of some tethered enzyme, of which the chloroacetyl warhead reacted with other nucleophilic amino acid residues. In this case, the tethered E2 variant may remain catalytically functional, leading to formation of polyubiquitin chains. Further investigation in the origin of such “leakiness” would set a stronger basis for development of this strategy. Nevertheless, the experiment was repeated several times to confirm the observed inhibition of UBE2L3*(89-**1**) by **7** (Supplementary Figure 4). Although bands corresponding to polyubiquitin chains were observed in some instances, in all cases, the level of polyubiquitination level was markedly less than the control groups.

One concern of applying this chemogenetic approach in cells is the high concentration of glutathione in human blood and cells (*ca.* 0.5 to 10 mM).[32,33] Nevertheless, the low reactivity of the proximity-dependent thiol-reactive warheads ($k = 10^{-2}$ to $10^{-3}$ $M^{-1}$ $s^{-1}$)[12] should preclude their intermolecular reactions with thiol-containing molecules in the environments. Indeed, conjugate **7** seemed to be stable in the presence of 0.5 to 50 mM glutathione (Supplementary Figure 5).

For cellular applications, conjugates have to be cell permeable. However, neither **6** nor **7** seemed to be cell permeable despite many conjugates containing a 3-phenyl-1,2,4,5-tetrazine motif are known to be.[14] In fact, **6** is structurally similar to the cell permeable MEK1/2 inhibitor conjugate **9** (Supplementary Figure 7). Conjugates **6** and **9** have the identical bioorthogonal functionality connected to a heptanoic acid or hexanoic acid linker, respectively. Thus, we were surprised that **6** could not label MEK1 variants containing either a cyclopropene or bicyclo[6.1.0]nonyne functionality. While it is disappointing that the conjugates are unlikely to be cell permeable, they can still be used for selective inhi-

bition of extracellular cysteine-dependent enzymes, such as cysteine cathepsins that have been associated with different diseases.[34] Nevertheless, it is likely that appendage of an aromatic ring to **6** to increase the hydrophobicity may render the molecule cell permeable, and this is a critical direction for future exploration.

This chemogenetic approach can theoretically be applied to any of the hundreds of cysteine-dependent enzymes, such as proteases, phosphatases, oxidoreductases, isomerases and ligases. Once established, the approach can also be easily extended to other enzymes within the same family, as exemplified with UBE2D1. Combining this approach with gene editing could allow for interesting research where genomically encoded proteins are altered to allow for rapid and selective modulation of their activity. This should be valuable for discerning the biological roles of enzymes where no selective small-molecule modulators are available.

### Materials and Methods

Amino acid **1** was purchased from Sirius Fine Chemicals (#SC-8017).

### Chemical synthesis of conjugates 2-8

*Tert*-**butyl (6-((4-(1,2,4,5-tetrazin-3-yl)benzyl)amino)-6-oxohexyl)carbamate (2).** A mixture of (4-(1,2,4,5-tetrazin-3-yl)phenyl)methanamine hydrochloride (5.0 mg, 22 μmol, 1.0 eq), Boc-6-aminohexanoic acid (6.7 mg, 29 μmol, 1.3 eq), EDC hydrochloride (8.6 mg, 45 μmol, 2.0 eq), HOBt (0.5 mg, 4 μmol, 0.15 eq) and dry pyridine (50 μL, 620 μmol, 28 eq) was stirred at room temperature until TLC analysis (DCM, 10% MeOH, $R_f \approx 0.5$) indicating complete consumption of the tetrazine starting material. The mixture was diluted with 5 mL of deionized water and extracted with EtOAc (3 × 10 mL). The combined organic phases are dried over $MgSO_4$ and filtered. The filtrate was evaporated under reduced pressure. The pink residue was subjected to two successive column chromatographies ($SiO_2$, $Et_2O$ to 2% MeOH in DCM, collecting only pink fractions to remove residual DMF; then reverse phase HPLC) to afford the tetrazine conjugate as pink solid (4.9 mg, 12 μmol, 56% yield). $^1$H NMR (400 MHz, $CDCl_3$): δ = 1.35–1.41 (m, 2H), 1.43 (s, 9H), 1.47–1.55 (m, 2H), 1.68–1.76 (m, 2H), 2.28 (t, *J* = 7.6 Hz, 2H), 3.11 (q, *J* = 6.2 Hz, 2H), 4.55 (brs, 1H), 4.57 (d, *J* = 5.8 Hz, 2H), 5.98 (brs, 1H), 7.51 (d, *J* = 8.0 Hz, 2H), 8.59 (d, *J* = 8.0 Hz, 2H), 10.21 (s, 1H); $^{13}$C NMR (100 MHz, $CDCl_3$): δ = 25.4, 26.5, 28.6, 29.9, 36.6, 40.4, 43.3, 79.3, 128.7, 128.8, 130.9, 144.2, 156.2, 158.0, 166.4, 173.0; ESI-(+)-HRMS (m/z): $[M+H]^+$ calcd. for $C_{20}H_{29}N_6O_3$, 401.2301; found, 401.2288.

**(*E*)-3-((4-Hydroxybutyl)thio)acrylonitrile (3a).** To a solution of (*E*)-3-tosylacrylonitrile (207 mg, 1.00 mmol, 1.0 eq) in $CH_2Cl_2$ (5.0 mL) was added 4-mercaptobutanol (125 μL, 1.20 mmol, 1.2 eq) and triethylamine (110 μL, 0.80 mmol, 0.8 eq) at room temperature. After stirring overnight, the solution volatiles were evaporated under reduced pressure and the residue was purified by column chromatography on silica (*n*-hexanes/EtOAc 2:1 to 1:1), which afforded acrylonitrile **3a** (139 mg, 0.88 mmol, 88%) as a slightly yellow oil**.** $^1$H NMR (400 MHz, $CDCl_3$): δ = 1.63–1.83 (m, 5H), 2.83 (t, *J* = 7.3 Hz, 2H), 3.68 (t, *J* = 6.1 Hz, 2H), 5.17 (d, *J* = 15.8 Hz, 1H), 7.35 (d, *J* = 15.8 Hz, 1H); $^{13}$C NMR (75 MHz, $CDCl_3$): δ = 25.1, 31.4, 31.9, 62.0, 91.4, 117.7, 152.1; EI-HRMS (m/z): $[M]^+$ calcd. for $C_7H_{11}NOS$, 157.0561; found, 157.0559.

**(*E*)-3-((4-(((4-Nitrophenoxy)carbonyl)oxy)butyl)thio)acrylonitrile (3b).** To a solution of (*E*)-3-((4-hydroxybutyl)thio)acrylonitrile (**3a**, 36 mg, 0.23 mmol, 1.0 eq) and pyridine (24 μL, 0.30 mmol, 1.3 eq) in $CH_2Cl_2$ (1.0 mL) 4-nitrophenylchloroformate (49 mg, 0.24 mmol, 1.1 eq) was added in portions. The solution was stirred at room temperature for 3 h, DIPEA (52 μL, 0.30 mmol, 1.3 eq) was added and the solution stirred for 20 h. The volatiles were evaporated and the residue was subjected to column chromatography on silica gel (*c*-hexane/EtOAc 4:1 to 1:1). Due to decomposition during column chromatography, carbonate **3b** was obtained as mixture with 4-nitrophenol as yellow oil in a 4:1 ratio (45 mg, 0.14 mmol, 61%). $^1$H NMR (300 MHz, $CDCl_3$): δ = 1.73–2.07 (m, 4H), 2.87 (t, *J* = 7.3 Hz, 2H), 4.32 (t, *J* = 6.1 Hz, 2H), 5.21 (d, *J* = 15.8 Hz, 1H), 7.34–7.49 (m, 3H), 8.28 (d, *J* = 8.2 Hz, 2H); $^{13}$C NMR (75 MHz, $CDCl_3$): δ = 25.0, 27.6, 31.7, 68.5, 91.9, 117.5, 121.9, 125.5, 145.5, 152.1, 152.6, 155.5; AP-(+)-HRMS (m/z): $[M+H]^+$ calcd. for $C_{14}H_{15}N_2O_5S$, 323.0692; found, 323.0702.

**(*E*)-3-((4-(((4-(1,2,4,5-Tetrazin-3-yl)benzyl)carbamoyl)oxy)butyl)thio)acrylonitrile (3).** To a solution of (*E*)-3-((4-(((4-citrophenoxy)carbonyl)oxy)butyl)thio)acrylnitrile (**3b**, 10.4 mg (4:1 mixture with 4-nitrophenol), 45 μmol, 1.3 eq) and (4-(1,2,4,5-tetrazin-3-yl)phenyl)methanamine hydrochloride (5 mg, 22 μmol, 1.0 eq) in dry $CH_2Cl_2$ (1.0 mL) was added dry pyridine (50 μL, 620 μmol, 28 eq). The solution was stirred for 20 h at room temperature. DIPEA (52 μL, 0.30 mmol, 1.3 eq) was added and the solution stirred for 24 h. The volatiles were evaporated and the pink residue was subjected to two successive column chromatographies ($SiO_2$, $Et_2O$ to 2% MeOH in DCM, collecting only pink fractions to remove residual DMF; then $SiO_2$, DCM to 2% MeOH in DCM) to afford the respective conjugate as pink solid. The pink residue was additionally subjected to reverse phase HPLC to afford the title compound **3** as pink solid (1.3 mg, 3.6 μmol, 16% yield). $^1$H NMR (500 MHz, $CDCl_3$): δ = 1.73–1.82 (m, 4H), 2.80–2.87 (m, 2H), 4.17 ($m_c$, 2H), 4.51 (d, *J* = 4.3 Hz, 2H), 5.13 (brs, 1H), 5.18 (d, *J* = 15.9 Hz, 1H), 7.34 (d, *J* = 15.8 Hz, 1H), 7.54 (d, *J* = 7.3 Hz, 2H), 8.61 (d, *J* = 7.5 Hz, 2H), 10.22 (s, 1H); $^{13}$C NMR (125 MHz, $CDCl_3$): δ = 25.2, 28.2, 31.8, 44.9, 64.3, 91.9, 117.6, 128.4, 128.8, 131.0, 144.2, 151.8, 156.7, 158.0, 166.4; ESI-(+)-HRMS (m/z): $[M+H]^+$ calcd. for $C_{17}H_{19}N_6O_2S$, 371.1290; found, 371.1296.

**Methyl (*E*)-3-((4-hydroxybutyl)thio)acrylate (4a).** To a solution of (*E*)-methyl 3-tosylacrylate[35] (600 mg, 2.50 mmol, 1.0 eq) in $CH_2Cl_2$ (15.0 mL) was added 4-mercaptobutanol (310 μL, 3.00 mmol, 1.2 eq) and triethylamine (280 μL, 2.02 mmol, 0.8 eq) at room temperature. After stirring for 3.5 h the solution was purified by column chromatography on silica (*n*-hexanes/EtOAc 4:1 to 1:1), which afforded **4a** (380 mg, 2.00 mmol, 80%) as a slightly yellow oil**.** $^1$H NMR (400 MHz, $CDCl_3$): δ = 1.74 ($m_c$, 4H), 2.84 (t, *J* = 7.2 Hz, 2H), 3.68 (t, *J* = 6.2 Hz, 2H), 3.72 (s, 3H), 5.75 (d, *J* = 15.2 Hz, 1H), 7.69 (d, *J* = 15.2 Hz, 1H); $^{13}$C NMR (100 MHz, $CDCl_3$): δ = 25.2, 31.7, 31.9, 51.6, 62.3, 113.5, 147.2, 166.0; EI-HRMS (m/z): $[M]^+$ calcd. for $C_8H_{14}O_3S$, 190.0664; found, 190.0661.

**Methyl (*E*)-3-((4-(((4-nitrophenoxy)carbonyl)oxy)butyl)thio)acrylate (4b).** To a solution of methyl (*E*)-3-((4-hydroxybutyl)thio)acrylate (**4a**, 118 mg, 0.62 mmol, 1.0 eq) and *N*,*N*-diisopropylethylamine (110 μL, 0.63 mmol, 1.0 eq) in $CH_2Cl_2$ (1.0 mL) 4-nitrophenylchloroformate (300 mg, 1.49 mmol, 2.4 eq) was added in portions. The yellow solution was stirred at room temperature for 16 h and directly subjected to column chromatography on silica gel (*n*-hexanes/EtOAc 9:1 to 1:1) without further work-up. Carbonate **4b** was obtained as yellow oil (118 mg, 0.33 mmol, 53%). $^1$H NMR (400 MHz, $CDCl_3$): δ = 1.79–1.92 (m, 4H), 2.85 (t, *J* = 6.9 Hz, 2H), 3.70 (s, 3H), 4.30 (t, *J* = 6.0 Hz, 2H), 5.75 (d, *J* = 15.2 Hz, 1H), 7.36 ($m_c$, 2H), 7.66 (d, *J* = 15.2 Hz, 1H), 8.26 ($m_c$, 2H); $^{13}$C NMR (100 MHz, $CDCl_3$): δ = 25.1, 27.6, 31.5, 51.6, 68.7, 113.7, 121.9, 125.4, 145.4, 146.8, 152.5, 155.5, 165.9; ESI-(+)-HRMS (m/z): $[M+Na]^+$ calcd. for $C_{15}H_{17}NNaO_7S$, 378.0623; found, 378.0610.

**Methyl (*E*)-3-((4-(((4-(1,2,4,5-tetrazin-3-yl)benzyl)carbamoyl) oxy)butyl)thio)acrylate (4).** To a solution of methyl (E)-3-((4 -(((4-nitrophenoxy)carbonyl)oxy)butyl)thio)acrylate (**4b**, 31 mg, 87 μmol, 1.9 eq) in dry DMF (1.0 mL) was added (4-(1,2,4,5-tetra zin-3-yl)phenyl)methanamine hydrochloride (10 mg, 45 μmol, 1.0 eq) and dry pyridine (43 μL, 533 μmol). The solution was stirred for 20 h at room temperature. The mixture was diluted with 5 mL of deionised water and extracted with EtOAc (3 × 10 mL). The combined organic phases were dried over $MgSO_4$ and the solvent was evaporated under reduced pressure. The pink residue was subjected to column chromatography ($SiO_2$, 20% EtOAc in *n*-hexanes), followed by reverse phase HPLC to afford the title compound **4** as pink solid. $^1$H NMR (500 MHz, $CDCl_3$): δ = 1.75–1.84 (m, 4H), 2.81–2.87 (m, 2H), 3.71 (s, 3H), 4.17 ($m_c$, 2H), 4.51 (d, *J* = 6.1 Hz, 2H), 5.29 (brs, 1H), 5.79 (d, *J* = 15.1 Hz, 1H), 7.54 (d, *J* = 8.1 Hz, 2H), 7.69 (d, *J* = 15.2 Hz, 1H), 8.61 (d, *J* = 8.3 Hz, 2H), 10.22 (s, 1H); $^{13}$C NMR (126 MHz, $CDCl_3$): δ = 25.3, 28.1, 31.6, 44.9, 51.6, 64.4, 113.7, 128.4, 128.8, 130.9, 144.3, 147.0, 156.8, 158.0, 166.0, 166.4; ESI-(+)-HRMS (m/z): [M +Na]$^+$ calcd. for $C_{18}H_{21}N_5NaO_4S$, 426.1207; found, 426.1201.

***N*-(4-(1,2,4,5-tetrazin-3-yl)benzyl)-6-(2-chloroacetamido)hex anamide (5).** (4-(1,2,4,5-tetrazin-3-yl)phenyl)methanamine hydrochloride (5.0 mg, 22 μmol, 1.0 eq), 6-[(chloroacetyl)amin o]hexanoic acid (6.0 mg, 29 μmol, 1.3 eq), EDC hydrochloride (8.6 mg, 45 μmol, 2.0 eq), HOBt (0.5 mg, 4 μmol, 0.15 eq), and dry pyridine (50 μL, 620 μmol, 28 eq) were stirred at room temperature until TLC analysis (DCM, 10% MeOH, $R_f \approx 0.5$) indicating complete consumption of the tetrazine starting material. The mixture was diluted with 5 mL of deionized water and extracted with EtOAc (3 × 10 mL). The combined organic phases are dried over $MgSO_4$ and filtered. The filtrate was evaporated under reduced pressure. The pink residue was subjected to two successive column chromatographies ($SiO_2$, $Et_2O$to 2% MeOH in DCM, collecting only pink fractions to remove residual DMF; then reverse phase HPLC) to afford the tetrazine conjugate **5** as pink solid (1.3 mg, 3.4 μmol, 15% yield). $^1$H NMR (400 MHz, $CDCl_3$): δ = 1.36–1.45 (m, 2H), 1.54–1.63 (m, 2H), 1.70–1.79 (m, 2H), 2.30 (t, *J* = 7.4 Hz, 2H), 3.33 (q, *J* = 6.7 Hz, 2H), 4.03 (s, 2H), 4.58 (d, *J* = 6.0 Hz, 2H), 5.91 (brs, 1H), 6.63 (brs, 1H), 7.52 (d, *J* = 8.0 Hz, 2H), 8.60 (d, *J* = 8.0 Hz, 2H), 10.22 (s, 1H); $^{13}$C NMR (100 MHz, $CDCl_3$): δ = 25.1, 26.4, 29.9, 36.5, 39.6, 42.8, 43.4, 128.7, 128.8, 130.9, 144.2, 158.0, 166.0, 166.4, 172.9; ESI-(+)-HRMS (m/z): [M+H]$^+$ calcd. for $C_{17}H_{22}N_6O_2Cl$, 377.1493; found, 377.1478.

**7-(2-chloroacetamido)heptanoic acid (6a).** To a biphasic mixture containing 7-aminoheptanoic acid (290.4 mg, 2.0 mmol, 1.0 eq) in 10 mL of DCM and aqueous solution of NaOH (1.0 M), a solution of 2-chloroacetyl chloride (175 μL, 2.2 mmol, 1.1 eq) in 2 mL DCM was added. After stirring for 3 h at RT, the aqueous phase was acidified to pH ∼ 2 with an aqueous solution of 1.0 M HCl. The mixture was extracted with DCM (3 × 10 mL). The organic phase was washed with water and brine, dried over $MgSO_4$ and filtered. The solvent was evaporated under reduced pressure to provide the product **6a** as a white solid (309 mg, 1.4 mmol, 70% yield), which was used without further purification. $^1$H NMR (400 MHz, $CDCl_3$): δ = 1.35–1.40 (m, 4H), 1.63–1.66 (m, 4H), 2.31–2.37 (m, 2H), 3.27–3.33 (m, 2H), 4.06 (s, 2H), 6.63 (brs, 1H); $^{13}$C NMR (100 MHz, $CDCl_3$): δ = 24.5, 26.4, 28.6, 29.1, 33.9, 39.8, 42.7, 166.2, 179.0; ESI-(+)-HRMS (m/z): [M-H]$^+$ calcd. for $C_9H_{15}NO_3Cl$, 220.0740; found, 220.0736.

***N*-(4-(1,2,4,5-tetrazin-3-yl)benzyl)-7-(2-chloroacetamido)hep tanamide (6).** To a solution of (4-(1,2,4,5-Tetrazin-3-yl)phenyl) methanamine hydrochloride (22 mg, 0.10 mmol, 1.0 eq), 6-[(chloroacetyl) amino] hexanoic acid (29 mg, 0.13 mmol, 1.3 eq), EDC hydrochloride (38 mg, 0.20 mmol, 2.0 eq), HOBt (2 mg, 0.015 mmol, 0.15 eq) in dry DMF (2.0 mL) was added dry pyridine (226 μL, 2.8 mmol, 28 eq) were stirred at room temperature for 16 h. The mixture was diluted with 5 mL of deionized water and extracted with EtOAc (3 × 10 mL). The combined organic phases are dried over $MgSO_4$ and filtered. The filtrate was evaporated under reduced pressure. The pink residue was subjected to two successive column chromatographies ($SiO_2$, 50% EtOAc in petroleum ether, then reverse phase HPLC) to afford the tetrazine conjugate **6** as pink solid (6.0 mg, 15 μmol, 15% yield). $^1$H NMR (600 MHz, $CDCl_3$): δ = 1.38–1.39 (m, 4H), 1.54–1.58 (m, 2H), 1.68–1.73 (m, 2H), 2.27 (t, *J* = 7.5 Hz, 2H), 3.30 (q, *J* = 6.8 Hz, 2H), 4.04 (s, 2H), 4.58 (d, *J* = 6.0 Hz, 2H), 5.95 (brs, 1H), 6.59 (brs, 1H), 7.52 (d, *J* = 8.1 Hz, 2H), 8.60 (d, *J* = 8.1 Hz, 2H), 10.22 (s, 1H); $^{13}$C NMR (100 MHz, $CDCl_3$): δ = 24.7, 26.4, 28.3, 29.2, 37.3, 39.6, 42.3, 43.2, 128.6, 128.7, 130.8, 142.9, 156.0, 164.9, 167.4, 171.8; ESI-(+)-HRMS (m/z): [M+H]$^+$ calcd. for $C_{18}H_{24}N_6O_2Cl$, 391.1649; found, 391.1625.

**2-Chloro-*N*-(2-(2-hydroxyethoxy)ethyl)acetamide (7a).** Aminoethoxy ethanol (2.05 g, 19.5 mmol, 1.0 eq) was dissolved in deionized water (20 mL) and THF (50 mL), cooled to 0 °C, and MgO (3.93 g, 97.5 mmol, 5.0 eq) was added. After stirring for 45 min, chloroacetyl chloride (1.5 mL, 19.5 mmol, 1.0 eq) in THF (20 mL), was added dropwise to the slurry while keeping the internal temperature below 10 °C. After stirring for 3 h at room temperature, the precipitate was filter off, and the solvent was removed to afford acetamide **7a** (3.33 g, 18.3 mmol, 94% yield) as yellowish oil, which was used without further purification.

**2-(2-(2-Chloroacetamido)ethoxy)ethyl (4-nitrophenyl) carbonate (7b).** To a solution of 2-chloro-*N*-(2-(2-hydroxye thoxy)ethyl)acetamide (**7a**, 180 mg, 1.00 mmol, 1.0 eq) and pyridine (100 μL, 1.00 mmol, 1.0 eq) in DMF (10.0 mL), 4-nitrophenylchloroformate (205 mg, 1.00 mmol, 1.0 eq) was added in portions. The yellow solution was stirred at room temperature for 16 h and partitioned between deionized water (100 mL) and EtOAc (100 mL). The phases were separated, the aqueous phase was extracted with EtOAc (3 × 50 mL), and the combined organic phases were washed with NaOH (1.0 M), deionized water, and brine. After drying with $MgSO_4$ and evaporation of the organic solvent under reduced pressure to give crude **7b** (330 mg, 0.953 mmol, 95% yield), which was used without further purification.

**2-(2-(2-Chloroacetamido)ethoxy)ethyl (4-(1,2,4,5-tetrazin-3-yl)benzyl)carbamate (7).** To a solution of 2-(2-(2-chloroaceta mido)ethoxy)ethyl (4-nitrophenyl) carbonate (**7b**, 10 mg, 29 μmol, 1.3 eq) and (4-(1,2,4,5-tetrazin-3-yl)phenyl)methana mine hydrochloride (5 mg, 22 μmol, 1.0 eq) in dry DMF (1.0 mL) was added dry pyridine (50 μL, 620 μmol, 28 eq). The solution was stirred for 20 h at room temperature. The mixture was diluted with 10 mL of deionized water and extracted with EtOAc (4 × 20 mL). The combined organic phases were dried over $MgSO_4$, and the solvent was evaporated under reduced pressure. The pink residue was subjected to two successive column chromatographies ($SiO_2$, $Et_2O$ to 2% MeOH in DCM, collecting only pink fractions to remove residual DMF; then $SiO_2$, DCM to 2% MeOH in DCM) to afford the respective conjugate as pink solid. The pink residue was subjected additionally subjected to reverse phase HPLC to afford the title compound **7** as pink solid (0.9 mg, 2.4 μmol, 11% yield). $^1$H NMR (500 MHz, $CDCl_3$): δ = 3.52 (q, *J* = 4.8 Hz, 2H), 3.62 (t, *J* = 4.8 Hz, 2H), 3.71 (t, *J* = 4.0 Hz, 2H), 4.04 (s, 2H), 4.30 (t, *J* = 3.8 Hz, 2H), 4.51 (d, *J* = 6.1 Hz, 2H), 5.27 (brs, 1H), 6.96 (brs, 1H), 7.54 (d, *J* = 8.0 Hz, 2H), 8.61 (d, *J* = 8.0 Hz, 2H), 10.22 (s, 1H); $^{13}$C NMR (125 MHz, $CDCl_3$): δ = 39.7, 42.8, 44.9, 64.3, 69.4, 69.6, 128.4, 128.8, 131.0, 144.1, 156.6, 158.0, 166.1, 166.4; ESI-(+)-HRMS (m/z): [M+H]$^+$ calcd. for $C_{16}H_{20}ClN_6O_4$, 395.1235; found, 395.1220.

**Methyl 6-propiolamidohexanoate (8a).** Methyl 6-aminohexanoate (370 mg, 2.5 mmol, 1.0 eq) and DCC (580 mg, 2.8 mmol, 1.1 eq) were dissolved in $CH_2Cl_2$. DIPEA (662 μL, 3.8 mmol, 1.5 eq) was added, and the reaction mixture was stirred at room temperature for 16 h. The white precipitate was removed by filtration, and the organic solvent was removed under reduced pressure. Column chromatography of the residue

on silica gel (cyclohexane/EtOAc 4:1 to 1:1) afforded the title compound **8a** as yellow oil (179 mg, 0.9 mmol, 36% yield). $^1$H NMR (400 MHz, $CDCl_3$): $\delta$ = 1.32–1.41 (m, 2H), 1.50–1.59 (m, 2H), 1.60–1.69 (m, 2H), 2.28 (t, *J* = 7.6 Hz, 2H), 2.78 (s, 1H), 3.29 (p, *J* = 6.8 Hz, 2H), 3.66 (s, 3H), 6.12 (brs, 1H); $^{13}$C NMR (100 MHz, $CDCl_3$): $\delta$ = 24.5, 26.3, 29.0, 33.9, 39.7, 51.7, 73.2, 77.4, 152.3, 174.1; ESI-(+)-HRMS (m/z): $[M+H]^+$ calcd. for $C_{10}H_{16}NO_3$, 198.1125; found, 198.1132.

**6-Propiolamidohexanoic acid (8b).** Methyl 6-propiolamidohexanoate (33 mg, 170 μmol, 1.0 eq) was dissolved in a mixture of deionized water/THF (1:1, 2.0 mL) and lithium hydroxide monohydrate (7 mg, 170 μmol,1.0 eq) was added. The mixture was stirred at room temperature until full conversion of the starting material was indicated by TLC. The mixture was brought to pH 3–4 using 1 M HCl. The phases were separated and the aqueous phase was extracted with EtOAc (5 × 10 mL). After drying over $Na_2SO_4$, the solvent was removed under reduced pressure to give crude **8b** as colourless oil (30 mg, 160 μmol, 98% yield), which was used without further purification.

***N*-(4-(1,2,4,5-Tetrazin-3-yl)benzyl)-6-propiolamidohexanamide (8).** (4-(1,2,4,5-Tetrazin-3-yl)phenyl)methanamine hydrochloride (3.0 mg, 13 μmol, 1.0 eq), 6-aminohexanoic acid derivative **8b** (5.3 mg, 29 μmol, 2.2 eq), EDC hydrochloride (8.6 mg, 45 μmol, 3.5 eq), HOBt (0.5 mg, 4 μmol, 0.30 eq) and dry pyridine (50 μL, 620 μmol, 48 eq) were stirred at room temperature until TLC analysis (DCM, 10% MeOH, $R_f \approx 0.5$) indicating complete consumption of the tetrazine starting material. The mixture was diluted with 5 mL of deionized water and extracted with EtOAc (3 × 10 mL). The combined organic phases are dried over $MgSO_4$ and filtered. The filtrate was evaporated under reduced pressure. The pink residue was subjected to two successive column chromatographies ($SiO_2$, $Et_2O$ to 2% MeOH in DCM, collecting only pink fractions to remove residual DMF; then reverse phase HPLC) to afford the tetrazine conjugate **8** as pink solid (0.5 mg, 1.3 μmol, 10% yield). $^1$H NMR (500 MHz, $CDCl_3$): $\delta$ = 1.37–1.45 (m, 2H), 1.54–1.63 (m, 2H), 1.73 (p, *J* = 7.5 Hz, 2H), 2.29 (t, *J* = 7.1 Hz, 2H), 2.77 (s, 1H), 3.33 (q, *J* = 6.6 Hz, 2H), 4.58 (d, *J* = 5.9 Hz, 2H), 5.91 (brs, 1H), 5.98 (brs, 1H), 7.52 (d, *J* = 8.0 Hz, 2H), 8.60 (d, *J* = 8.0 Hz, 2H), 10.22 (s, 1H); $^{13}$C NMR (125 MHz, $CDCl_3$): $\delta$ = 25.0, 26.3, 29.0, 36.4, 39.6, 43.4, 73.2, 128.7, 128.9, 130.9, 144.1, 158.0, 166.4, 172.9; ESI-(+)-HRMS (m/z): $[M+H]^+$ calcd. for $C_{18}H_{21}N_6O_2$, 353.1726; found, 353.1733.

## Cloning

The gene encoding for HOIP(697-1072) with an N-terminal hexa-histidine tag (His tag) was purchased as a gene fragment from ThermoFisher (GeneArt Strings). A tobacco etch virus (TEV) protease recognition site (ENLYFQG) was included between the hexa-histidine tag and the HOIP to allow for its cleavage. This fragment was cloned into the NdeI and EcoRI sites of a pET28a vector.

Plasmids encoding UBE2L3* and UBE2L3*(XX-**1**) containing an N-terminal His tag were constructed by the Cloning Department at the MRC PPU. Plasmids encoding the UBE2L3 and UBE2L3 (89-**1**) were obtained via site-directed mutagenesis to reintroduce C17 and C137.

The gene encoding for UBE2D1 with an N-terminal His tag was purchased as a gene fragment from ThermoFisher (GeneArt Strings). This fragment was cloned into the XbaI and NotI sites of a pET15b vector. Variant UBE2D1(88-**1**) was constructed by site-directed mutagenesis.

## Protein expression and purification

His tagged HOIP(697-1072) was expressed in *E. coli* BL21(DE3) pLysS cells by induction with isopropyl-1-thio-β-D-galactopyrano side (IPTG, 0.4 mM) and supplemented with $ZnCl_2$ (0.1 mM) when cultures reached an optical density at 600 nm ($OD_{600}$) of 0.6. Cultures were incubated at 16 °C overnight before harvesting the cells. Cell pellets were resuspended in 50 mM Tris-HCl pH 8.0, 2 mM imidazole, 1 μM $ZnCl_2$, 150 mM NaCl, 5 mM 2-mercaptoethanol supplemented with 1 mg/mL of lysozyme, 0.1 mM phenylmethylsulfonyl fluoride and 5 μM DNase before being lysed via sonication. Initial purification was carried out through Ni-NTA affinity chromatography. After concentrating protein fractions and exchanging the buffer for 20 mM Tris-HCl pH 7.4, 20 μM $ZnCl_2$, 200 mM NaCl, 5 mM citrate and 5 mM 2-mercaptoethanol, the His tag was cleaved by incubation with TEV protease, followed by an additional Ni-NTA affinity chromatography step.

UBE2L3 and UBE2D1 variants were expressed in in *E. coli* BL21 (DE3) cells by induction with IPTG (0.5 mM) when cultures reached an $OD_{600}$ of 0.6. For variants, addition of **1** (0.5 mM) was performed prior to induction, when cultures reached an $OD_{600}$ of 0.4. Cultures were incubated at 37 °C for 4 hours before harvesting the cells. Cell pellets were resuspended in 20 mM Tris-HCl pH 7.4, 25 mM imidazole, 150 mM NaCl supplemented with 1 mg/mL of lysozyme, 0.1 mM phenylmethylsulfonyl fluoride and 5 μM DNase before being lysed via sonication. Purification was carried out via Ni-NTA affinity chromatography.

## Polyubiquitination assays

Polyubiquitination reactions contained 1 μM UBE1, 5 μM UBE2L3 or UBE2D1, 5 μM HOIP(697-1072), 40 μM ubiquitin and finally 10 mM ATP combined in a buffered solution of 50 mM HEPES, 150 mM NaCl, 20 mM $MgCl_2$, pH 7.5. Reactions were then incubated at 37 °C for 3 hours, unless otherwise indicated, after which aliquots were taken, loading buffer (ThermoFisher, # NP0007) was added. The mixtures were heated at 95 °C for 5 minutes. Samples were loaded onto Novex™ 4–20% Tris-Glycine Mini Protein Gels, 15-well, WedgeWell™ format, for SDS-PAGE analysis.

## E2 inhibition assays

E2 enzymes were incubated with 50 μM (unless otherwise indicated) of **2**–**8** at 25 °C for 16 hours in a buffered solution of 50 mM HEPES, 150 mM NaCl, 20 mM $MgCl_2$, pH 7.5. The subsequent polyubiquitination assay was then carried out as described above, with the addition of E1, E3, ubiquitin and ATP. Samples were taken after incubation at 37 °C and analysed via SDS-PAGE.

## Mass spectrometry analysis

LC-MS was performed on a Waters Synapt G2-Si quadrupole time of flight mass spectrometer coupled to a Waters Acquity H-Class UPLC system. The column was an Acquity UPLC protein BEH C4 (300 Å 1.7 μm × 2.1 mm × 100 mm) operated in reverse phase and held at 60 °C. The gradient employed was 95% A to 35% A over 50 minutes, where A is 0.1% $HCO_2H_{(aq)}$ and B is 0.1% $HCO_2H$ in acetonitrile. Data was collected in positive electrospray ionization mode and analyzed using the Waters MassLynx software version 4.1. Deconvolution of protein charged states was obtained using the maximum entropy 1 processing software.

## Reaction of conjugate 7 with cyclopropene lysine, bicyclo[6.1.0]nonyne lysine or glutathione

Conjugate **7** (2.0 mg) was dissolved in 506 μL DMSO to make its 10 mM stock solution. Its 100 μM stock solution was prepared from mixing 10 μL solution of **7** (10 mM in DMSO), 90 μL

DMSO and 900 μL $H_2O$.
Cyclopropene lysine **1** (10.0 mg) or bicyclo[6.1.0]nonyne lysine **10** (10.0 mg) was dissolved in 390 μL or 310 μL of 100 mM NaOH, respectively, to afford their corresponding stock solutions at 100 mM. Their 100 μM stock solutions were prepared from diluting their 100 mM stock solutions for 1000 times.
Glutathione (10.0 mg) was dissolved in 325 μL 100 mM NaOH to make its 100 mM stock solution. Its 10 mM and 1 mM stock solutions were prepared from diluting the 100 mM stock solution for 10 and 100 times, respectively.
The reaction of 50 μM **7** and 5 μM **1** was performed by mixing **7** (100 μM, 100 μL), $H_2O$ (90 μL) and **1** (100 μM, 10 μL) in the described order. The reaction of 5 μM **7** and 5 μM **10** was performed by mixing **7** (100 μM, 10 μL), $H_2O$ (180 μL) and **1** (100 μM, 10 μL) in the described order. The reaction of 5 μM **7** and 0.5 mM glutathione was performed by mixing **7** (100 μM, 10 μL), $H_2O$ (90 μL) and glutathione (1 mM, 100 μL) in the described order. The reaction of 5 μM **7** and 5 mM glutathione was performed by mixing **7** (100 μM, 10 μL), $H_2O$ (90 μL) and glutathione (10 mM, 100 μL) in the described order. The reaction of 5 μM **7** and 50 mM glutathione was performed by mixing **7** (100 μM, 10 μL), $H_2O$ (90 μL) and glutathione (100 mM, 100 μL) in the described order.
The reactions were monitored by UPLC-MS (10% to 100% acetonitrile over 7 minutes) at different time points. Data was collected at absorption wavelength of 254 nm and in positive or negative electrospray ionization mode, followed by analysis using the Waters MassLynx software version 4.1. Rate constant was calculated using the Fit ODE function in OriginPro2021.

### Cell permeability assays

HEK293T cells were co-transfected with plasmids encoding a constitutively active MEK1 variant with an amber codon at 76 position, a eGFP-ERK2 reporter and a corresponding aminoacyl-tRNA synthetase/tRNA pair for incorporation of **1** or bicyclo[6.1.0]nonyne lysine. Cells were cultured in the presence of 0.1 mM bioorthogonal amino acid for 24 h. Cells were then washed with PBS twice, followed by incubation with DMEM for 30 min to remove any unincorporated bioorthogonal amino acid. Cells were then subjected to treatment 1 in which cells were incubated with DMSO, **6**, **7** or **11** for 10 or 2 h. After the incubation, cells were washed with PBS twice to remove the conjugate, and then subjected to treatment 2 where the cells were incubated with or without conjugate **9**. Two hours post treatment 2, cells was collected for immunoblotting.
Cells were lysed using RIPA (Merck, R0278) with protease inhibitor cocktail (Yamei, GRF101). Equal volumes of sample were subjected to SDS-PAGE, followed by transferring to nitrocellulose membranes. Membranes were blocked with PBST containing 5% skim-milk for 1 h under room temperature and then overnight with HA (1:1000, ABclonal, AE008), GFP (1:1000, ABclonal, AE012) as well as Phospho-Erk1-T202/Y204 + Erk2-T185/Y187 (1:1000, ABclonal, AP0974) antibodies at 4 °C. After three washing steps, membranes were incubated with HRP-conjugates secondary antibodies (1:20000, ABclonal, AS014 or 1:20000, ABclonal, AS003) for 1 h at room temperature and visualized using a Bio-Rad ChemiDoc MP system.

## CRediT authorship contribution statement

**Luke A. Spear:** Methodology, Validation, Investigation, Writing – original draft, Writing – review & editing, Visualization. **Yang Huang:** Validation, Investigation, Writing – review & editing, Visualization. **Jinghao Chen:** Investigation, Writing – review & editing, Visualization. **Alexander R. Nödling:** Investigation, Writing – review & editing. **Satpal Virdee:** Conceptualization, Methodology, Investigation, Resources, Writing – review & editing, Supervision, Funding acquisition. **Yu-Hsuan Tsai:** Conceptualization, Writing – original draft, Writing – review & editing, Visualization, Supervision, Project administration, Funding acquisition.

## DECLARATION OF COMPETING INTEREST

The authors declare that they have no known competing financial interests or personal relationships that could have appeared to influence the work reported in this paper.

### Acknowledgements

We are grateful for the financial support from Biotechnology and Biological Sciences Research Council (BB/ P003982/1 to S.V.), Engineering and Physical Sciences Research Council (EP/N509449/1: 1928910 to LAS), Medical Research Council (MC_UU_12016/8 to S.V.) as well as Shenzhen Bay Laboratory (SZBL) and National Natural Science Foundation of China. We thank Dr. Kung Ching Cookson Chiu of the SZBL Mass Spectrometry Facility for assistance. We thank Axel Knebel and team members of the MRC PPU Protein Production and Assay Development facility for production of E1 activating enzyme. We thank Nicola T. Wood and members of the MRC PPU DNA Cloning Facility for design and production of DNA clones.

## Appendix A. Supplementary Data

Supplementary data to this article can be found online at https://doi.org/10.1016/j.jmb.2022.167524. Original pdf files of protein mass spectrometry results have been deposited to the Cardiff University data catalog at http://doi.org/10.17035/d.2022.0162081903.

*Received 20 August 2021;*
*Accepted 28 February 2022;*
*Available online 3 March 2022*

***Keywords***:
genetic code expansion;
non-canonical amino acid;
chemogenetics;
E2 ubiquitin-conjugating enzymes;
bioorthogonal reaction

***Abbreviations***:
DMSO, dimethyl sulfoxide; DCM, dichloromethane; DIPEA, *N*,*N*-diisopropylethylamine; DCC,

dicyclohexylcarbodiimide; EDC, 1-ethyl-(3-dimethylamino propyl)carbodiimide; THF, tetrahydrofuran; DMF, *N,N*-dimethylformamide; HOBt, 1-hydroxybenzotriazole

## References


1. Dhanwani, R., Takahashi, M., Sharma, S., (2018). Cytosolic sensing of immuno-stimulatory DNA, the enemy within. *Curr. Opin. Immunol.* **50**, 82–87.
2. Dantuma, N.P., Bott, L.C., (2014). The ubiquitin-proteasome system in neurodegenerative diseases: precipitating factor, yet part of the solution. *Front. Mol. Neurosci.* **7**
3. Sreedhar, A., Zhao, Y., (2018). Dysregulated metabolic enzymes and metabolic reprogramming in cancer cells. *Biomed. Rep.* **8**, 3–10.
4. Makin, S., (2018). The amyloid hypothesis on trial. *Nature* **559**, S4–S7.
5. Simon, G.M., Cravatt, B.F., (2010). Activity-based proteomics of enzyme superfamilies: serine hydrolases as a case study. *J. Biol. Chem.* **285**, 11051–11055.
6. Oprea, T.I., Bologa, C.G., Brunak, S., Campbell, A., Gan, G.N., Gaulton, A., et al., (2018). Unexplored therapeutic opportunities in the human genome. *Nat. Rev. Drug Discov.* **17**, 317–332.
7. Schreiber, S.L., Kotz, J.D., Li, M., Aube, J., Austin, C.P., Reed, J.C., et al., (2015). Advancing Biological Understanding and Therapeutics Discovery with Small-Molecule Probes. *Cell* **161**, 1252–1265.
8. Shogren-Knaak, M.A., Alaimo, P.J., Shokat, K.M., (2001). Recent advances in chemical approaches to the study of biological systems. *Annu. Rev. Cell Dev. Biol.* **17**, 405–433.
9. El-Brolosy, M.A., Stainier, D.Y.R., (2017). Genetic compensation: A phenomenon in search of mechanisms. *PLoS Genet.* **13**, e1006780.
10. Arrowsmith, C.H., Audia, J.E., Austin, C., Baell, J., Bennett, J., Blagg, J., et al., (2015). The promise and peril of chemical probes. *Nat. Chem. Biol.* **11**, 536–541.
11. Islam, K., (2018). The Bump-and-Hole Tactic: Expanding the Scope of Chemical Genetics. *Cell Chem. Biol.* **25**, 1171–1184.
12.. Tsai, Y.H., Doura, T., Kiyonaka, S., (2021). Tethering-based chemogenetic approaches for the modulation of protein function in live cells. *Chem. Soc. Rev.* **50**, 7909–7923.
13. Zheng, H., Al-Ayoubi, A., Eblen, S.T., (2010). Identification of novel substrates of MAP Kinase cascades using bioengineered kinases that uniquely utilize analogs of ATP to phosphorylate substrates. *Methods Mol. Biol.* **661**, 167–183.
14. Tsai, Y.-H., Essig, S., James, J.J., Lang, K., Chin, J.W., (2015). Selective rapid and optically switchable regulation of protein function in live mammalian cells. *Nat. Chem.* **7**, 554–561.
15. Morgan, C.W., Dale, I.L., Thomas, A.P., Hunt, J., Chin, J. W., (2021). Selective CRAF Inhibition Elicits Transactivation. *J. Am. Chem. Soc.* **143**, 4600–4606.
16. Lang, K., Chin, J.W., (2014). Bioorthogonal reactions for labeling proteins. *ACS Chem. Biol.* **9**, 16–20.
17. Schmied, W.H., Elsasser, S.J., Uttamapinant, C., Chin, J. W., (2014). Efficient Multisite Unnatural Amino Acid Incorporation in Mammalian Cells via Optimized Pyrrolysyl tRNA Synthetase/tRNA Expression and Engineered eRF1. *J. Am. Chem. Soc.* **136**, 15577–15583.
18. Stanley, M., Han, C., Knebel, A., Murphy, P., Shpiro, N., Virdee, S., (2015). Orthogonal thiol functionalization at a single atomic center for profiling transthiolation activity of E1 activating enzymes. *ACS Chem. Biol.* **10**, 1542–1554.
19. Oliveira, B.L., Guo, Z., Bernardes, G.J.L., (2017). Inverse electron demand Diels-Alder reactions in chemical biology. *Chem. Soc. Rev.* **46**, 4895–4950.
20. Karver, M.R., Weissleder, R., Hilderbrand, S.A., (2011). Synthesis and evaluation of a series of 1,2,4,5-tetrazines for bioorthogonal conjugation. *Bioconjug. Chem.* **22**, 2263–2670.
21. Steen, E.J.L., Jorgensen, J.T., Denk, C., Battisti, U.M., Norregaard, K., Edem, P.E., et al., (2021). Lipophilicity and Click Reactivity Determine the Performance of Bioorthogonal Tetrazine Tools in Pretargeted In Vivo Chemistry. *ACS Pharmacol. Transl. Sci.* **4**, 824–833.
22. Flanagan, M.E., Abramite, J.A., Anderson, D.P., Aulabaugh, A., Dahal, U.P., Gilbert, A.M., et al., (2014). Chemical and computational methods for the characterization of covalent reactive groups for the prospective design of irreversible inhibitors. *J. Med. Chem.* **57**, 10072–10079.
23. Zheng, X., Li, Z., Gao, W., Meng, X., Li, X., Luk, L.Y.P., et al., (2020). Condensation of 2-((alkylthio)(aryl) methylene)malononitrile with 1,2-aminothiol as a novel bioorthogonal reaction for site-specific protein modification and peptide cyclization. *J. Am. Chem. Soc.* **142**, 5097–5103.
24. Backus, K.M., Correia, B.E., Lum, K.M., Forli, S., Horning, B.D., Gonzalez-Paez, G.E., et al., (2016). Proteome-wide covalent ligand discovery in native biological systems. *Nature* **534**, 570–574.
25. Alpi, A.F., Chaugule, V., Walden, H., (2016). Mechanism and disease association of E2-conjugating enzymes: lessons from UBE2T and UBE2L3. *Biochem. J.* **473**, 3401–3419.
26. Huang, X., Dixit, V.M., (2016). Drugging the undruggables: exploring the ubiquitin system for drug development. *Cell Res.* **26**, 484–498.
27. Pao, K.C., Stanley, M., Han, C., Lai, Y.C., Murphy, P., Balk, K., et al., (2016). Probes of ubiquitin E3 ligases enable systematic dissection of parkin activation. *Nat. Chem. Biol.* **12**, 324–331.
28. Huang, L., Kinnucan, E., Wang, G., Beaudenon, S., Howley, P.M., Huibregtse, J.M., et al., (1999). Structure of an E6AP-UbcH7 complex: insights into ubiquitination by the E2–E3 enzyme cascade. *Science* **286**, 1321–1326.
29. Nodling, A.R., Spear, L.A., Williams, T.L., Luk, L.Y.P., Tsai, Y.-H., (2019). Using genetically incorporated unnatural amino acids to control protein functions in mammalian cells. *Essays Biochem.* **63**, 237–266.
30. de la Torre, D., Chin, J.W., (2021). Reprogramming the genetic code. *Nat. Rev. Genet.* **22**, 169–184.
31. Johansson, H., Isabella Tsai, Y.C., Fantom, K., Chung, C. W., Kumper, S., Martino, L., et al., (2019). Fragment-Based Covalent Ligand Screening Enables Rapid Discovery of Inhibitors for the RBR E3 Ubiquitin Ligase HOIP. *J. Am. Chem. Soc.* **141**, 2703–2712.
32. Scibior, D., Skrzycki, M., Podsiad, M., Czeczot, H., (2008). Glutathione level and glutathione-dependent enzyme activities in blood serum of patients with gastrointestinal tract tumors. *Clin. Biochem.* **41**, 852–858.

33. Meister, A., (1988). Glutathione metabolism and its selective modification. *J. Biol. Chem.* **263**, 17205–17208.
34. Vidak, E., Javorsek, U., Vizovisek, M., Turk, B., (2019). Cysteine Cathepsins and their Extracellular Roles: Shaping the Microenvironment. *Cells.* **8**, 264.
35. Katrun, P., Chiampanichayakul, S., Korworapan, K., Pohmakotr, M., Reutrakul, V., Jaipetch, T., et al., (2010). PhI(OAc)2/KI-Mediated Reaction of Aryl Sulfinates with Alkenes, Alkynes, and α, β-Unsaturated Carbonyl Compounds: Synthesis of Vinyl Sulfones and β-Iodovinyl Sulfones. *Eur. J. Org. Chem.* **2010**, 5633–5641.